Article

Cell Reports

AMP-Activated Protein Kinase Directly Phosphorylates and Destabilizes Hedgehog Pathway Transcription Factor GLI1 in Medulloblastoma

Graphical Abstract

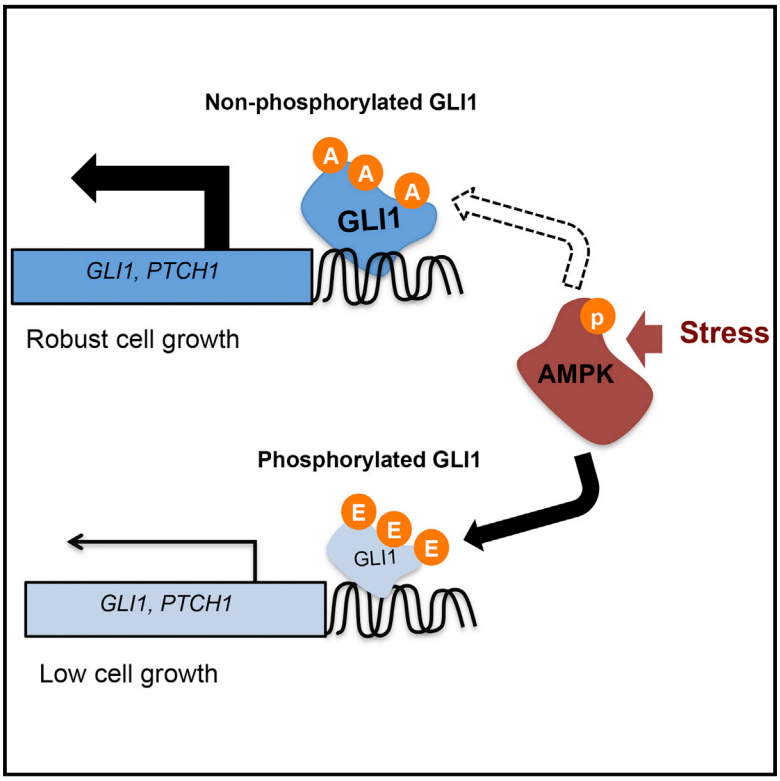

Authors

Yen-Hsing Li, Jia Luo, Yung-Yi C. Mosley, ..., Chun-Ju Chang, Matthew P. Scott, Jer-Yen Yang

Correspondence

jyyang@purdue.edu

In Brief

Li. et al. show that AMPK is linked to the Hh signaling pathway. Activation of AMPK phosphorylates GLI1, a Hedgehog transcriptional activator, and inhibits Hh activity. GLI1 phosphorylation decreases GLI1 protein stability and reduces cell growth, colony formation, and tumor growth in mice.

Highlights

- AMPK blocks Shh-induced transcriptional activity
- AMPK reduces GLI1 protein level and stability
- AMPK phosphorylates GLI1 at serines 102 and 408 and threonine 1074
- GLI1^{3A} protein is resistant to AMPK and has higher stability and oncogenic ability

Li et al., 2015, Cell Reports *12*, 599–609
July 28, 2015
http://dx.doi.org/10.1016/j.celrep.2015.06.054

Cell Reports
Article

AMP-Activated Protein Kinase Directly Phosphorylates and Destabilizes Hedgehog Pathway Transcription Factor GLI1 in Medulloblastoma

Yen-Hsing Li,[1] Jia Luo,[3] Yung-Yi C. Mosley,[1] Victoria E. Hedrick,[4] Lake N. Paul,[4] Julia Chang,[3] GuangJun Zhang,[2,5] Yu-Kuo Wang,[6] Max R. Banko,[7] Anne Brunet,[7] Shihuan Kuang,[2,8] Jen-Leih Wu,[9] Chun-Ju Chang,[1,2] Matthew P. Scott,[3] and Jer-Yen Yang[1,2,*]

[1]Department of Basic Medical Sciences
[2]Center for Cancer Research
Purdue University College of Veterinary Medicine, West Lafayette, IN 47907, USA
[3]Departments of Developmental Biology, Genetics, and Bioengineering, Stanford University School of Medicine, Stanford, CA 94305, USA
[4]Bindley Bioscience Center, Purdue University, West Lafayette, IN 47906, USA
[5]Department of Comparative Pathobiology, Purdue University College of Veterinary Medicine, West Lafayette, IN 47907, USA
[6]Department of Biological Science and Technology, National Chiao Tung University, Hsin-Chu 300, Taiwan
[7]Department of Genetics, Stanford University School of Medicine, Stanford, CA 94305, USA
[8]Department of Animal Sciences, Purdue University, West Lafayette, IN 47907, USA
[9]Institute of Cellular and Organismic Biology, Academia Sinica, Taipei 115 Taiwan
*Correspondence: jyyang@purdue.edu
http://dx.doi.org/10.1016/j.celrep.2015.06.054

SUMMARY

The Hedgehog (Hh) pathway regulates cell differentiation and proliferation during development by controlling the Gli transcription factors. Cell fate decisions and progression toward organ and tissue maturity must be coordinated, and how an energy sensor regulates the Hh pathway is not clear. AMP-activated protein kinase (AMPK) is an important sensor of energy stores and controls protein synthesis and other energy-intensive processes. AMPK is directly responsive to intracellular AMP levels, inhibiting a wide range of cell activities if ATP is low and AMP is high. Thus, AMPK can affect development by influencing protein synthesis and other processes needed for growth and differentiation. Activation of AMPK reduces GLI1 protein levels and stability, thus blocking Sonic-hedgehog-induced transcriptional activity. AMPK phosphorylates GLI1 at serines 102 and 408 and threonine 1074. Mutation of these three sites into alanine prevents phosphorylation by AMPK. This leads to increased GLI1 protein stability, transcriptional activity, and oncogenic potency.

INTRODUCTION

Regulation of energy production and storage is necessary for living organisms, especially during stages of development that involve substantial growth. Otherwise embryos may invest precious energy in starting organogenesis that cannot be completed. The problem is exemplified by the crucial function of mitochondria, which are the major source of ATP during human pre-implantation development (Wilding et al., 2009). Therefore, developmental control systems that guide the growth of organs and tissues must be coordinated with energy supply.

The Hedgehog (Hh) pathway is essential for the development of most organs and tissues. Loss of control of the pathway is oncogenic in tissues where a normal role of the Hh signal is to promote growth. Mutations that deregulate Hh signaling are associated with sporadic and familial skin cancer (basal cell carcinoma) and brain tumors (medulloblastoma). For example, Gorlin syndrome is due to loss-of-function mutations in the *PTCH* gene, which encodes the receptor protein Patched1 (Ptch) that binds Hh ligand. Normally Ptch protein restrains Hh transduction, and therefore growth of the skin and cerebellum, until it is inactivated by the Hh ligand; but, the tumor cells sense the loss of Ptch function and divide without the need for Hh signals. Given the fine line between mitogenesis and oncogenesis, appropriate regulation of developmental pathways is critical.

Hh signaling controls transcription of target genes by regulating activities of the three Glioma-associated oncogene (Gli1–3) transcription factors. When Hh ligand binds to the Ptch receptor, a 12-pass transmembrane protein, Ptch no longer inhibits the 7-transmembrane domain transducer Smoothened (Smo). In cells not exposed to Hh ligand, Ptch is resident in the plasma membrane overlying primary cilia (Rohatgi et al., 2007); Ptch moves into the cell and is degraded upon binding Hh. Activated Smo then accumulates in primary cilia, which are non-motile solitary appendages on many cell types and serve as transduction centers for Hh signals (Rohatgi et al., 2007). Activation of Smo antagonizes Sufu, a Gli1 negative regulator, to promote nuclear translocation of active Gli proteins and induction of genes that control cell proliferation or differentiation during development.

Embryos devote specific regulatory systems to conserving or increasing the energy supply during times of need. One crucial

energy-sensing molecule is AMP-activated protein kinase (AMPK). AMPK monitors cellular energy status by responding to AMP/ATP ratios, as well as AMP and ATP concentrations (Scott et al., 2009; Steinberg and Kemp, 2009). The levels of AMP and ATP reflect environmental nutrient supply and uptake. High AMP activates AMPK, which then inhibits energy-consuming processes such as protein synthesis, and boosts energy production by increasing glucose uptake and glycolysis (Hardie et al., 2012).

AMPK is a heterotrimer consisting of α, β, and γ subunits. AMPK is activated approximately 1,000-fold by phosphorylation of a conserved threonine (Thr172) in the activation loop of the KD by upstream protein kinases, such as serine/threonine kinase 11 (STK11, also known as Liver Kinase B1 [LKB1]) (Jishage et al., 2002). When AMP or ADP concentrations are high, their increased binding to the γ subunit causes a conformational change that promotes phosphorylation of Thr172 by LKB1 and inhibits dephosphorylation (Xiao et al., 2011). Genetic experiments show that zebrafish embryos do not require LKB1 if energy is abundant; but, in conditions of energy stress, LKB1 is essential for life (van der Velden et al., 2011). The kinase activity of mammalian phosphorylated AMPK can be enhanced 2- to 5-fold by the binding of AMP to its γ subunit (Sanders et al., 2007; Suter et al., 2006). ATP is an antagonist of AMPK activation, acting by binding to the γ subunit and competing with AMP or ADP binding (Hardie et al., 2012; Xiao et al., 2007).

Development cannot proceed if energy stores are inadequate. Slowing or postponing developmental steps may save the life of a growing animal. Hh signaling recently has been shown to trigger rapid glycolysis in adipocytes by modifying Smo activity, Ca^{2+} levels, and AMPK activity (Teperino et al., 2012). Thus, the Hh developmental pathway alters production of ATP. We have been investigating the complementary possibility that transduction through the Hh pathway is modulated by energy stores. When energy is scarce and cell division or cell differentiation should be slowed to conserve remaining stores, activated AMPK may indirectly affect developmental pathways like Hh by reducing protein synthesis or other basic gene expression functions. A second possibility is that a more direct regulatory connection links energy sensing with developmental regulators. We have investigated this second possibility using cultured cells that respond to Hh signaling proteins.

RESULTS

Control of Gli1 Protein Level and Stability by AMPK

To investigate whether AMPK regulates the Hh pathway, we used the NIH 3T3 cell line, a well-known Hh-responsive cell line. Cells were treated with the AMPK activator two-deoxyglucose (2DG), a glucose analog that blocks ATP production by inhibiting glycolysis and thereby induces AMPK activation (Wick et al., 1957). Activation of AMPK reduced Gli1 protein levels progressively over time (Figure 1A). As NIH 3T3 cells were treated for increasing numbers of hours with 2DG, the amount of activated AMPK (p-AMPK) increased. The amount of a direct AMPK substrate that is often used to measure AMPK activity (Henin et al., 1995), phospho-Acetyl-CoA Carboxylase (p-ACC), also increased for at least 4 hr. In addition to 2DG, similar effects were observed when two other AMPK activators (A769662 and AICAR) were applied to NIH 3T3 and pZp53Med1 (Med1) medulloblastoma cells (Figure 1B). In addition, protein levels of Gli2 and Gli3 (FL and R) did not change while AMPK was activated (Figure S1A). *AMPK* knockout MEF cells had increasing (1.71-fold) Gli1 protein compared to wild-type (WT) MEF, and the amount of Gli1 protein was low in $AMPK^{+/+}$ cells in the presence of 2DG and did not change in the $AMPK^{-/-}$ cells (Figure 1C). Therefore, the low level of Gli1 protein caused by 2DG administration was due to AMPK-dependent action.

Knocking down *Lkb1* dysregulates the Hh pathway by affecting Gli3 (Jacob et al., 2011). We found that two different *Lkb1* small hairpin RNAs (shRNAs) reduced the level of Lkb1 protein by half in Med1 cells, while the level of Gli1 protein was not affected (Figure S1B). In $Lkb1^{-/-}$ myoblast cells, both Gli1 protein and mRNA levels were not much different in comparison with $Lkb1^{+/+}$ cells (Figures S1C and S1D). When $Lkb1^{+/+}$ and $Lkb1^{-/-}$ cells were treated with AICAR, Gli1 protein level was reduced in both (Figure S1C). We conclude that Lkb1 is not involved in the AMPK-mediated reduction of the Gli1 protein levels. HEK293 cells were transfected with a kinase-dead *AMPK* mutant (Banko et al., 2011) that is unable to phosphorylate proteins. The result was an increase in the Gli1 protein level compared to cells transfected with WT AMPK (Figure 1D).

Gli1 is transcriptionally activated by Shh. Activating AMPK reduced Gli1 protein levels in NIH 3T3 cells despite stimulation with Shh ligand (Figure 1E). Co-treatment of the cells with 2DG and Shh increased the amount of activated AMPK measured as p-AMPK and its target p-ACC, and reduced the amount of Gli1 protein compared to cells treated with Shh alone. Med1 cells, which have constitutively active Hh target gene expression (Berman et al., 2002), also had reduced Gli1 protein levels in the presence of 2DG (Figure 1F). The reduction of Gli1 protein may have been due to protein degradation. Co-treatment with 2DG and proteasome inhibitor (MG132) restored the higher amount of Gli1 protein (Figure S1E). This indicates that, even upon stimulation by Shh, which increases the amount of Gli1 protein because *Gli1* is a transcriptional target, activated AMPK is able to reduce Gli1 protein levels.

The reduction of the Gli1 protein level by activated AMPK could be due to an effect on *Gli1* transcription, translation, or post-translational stability. We find that Gli1 protein stability is altered by the activity state of AMPK. We used cycloheximide (CHX) to block translation of new protein and monitored the stability of pre-existing Gli1 protein. When AMPK was functional (Figure 1G, left), the amount of Gli1 protein decreased with a half-life of 4 hr. In cells lacking AMPK (Figure 1G, right), Gli1 protein remained stable with a half-life of at least 8 hr. Gli1 instability was accelerated in 2DG and CHX co-treated $AMPK^{+/+}$ cells (Figure 1H), but was not affected in $AMPK^{-/-}$ cells (Figure 1H). The protein stabilities of Gli2 and Gli3 were not affected in the 2DG and CHX co-treated Med1 cells (Figure S1F). In this experiment AMPK could not have been affecting synthesis of Gli1, which was prevented, but instead affected Gli1 protein stability.

AMPK Reduces Gli1 Transcriptional Activity

We tested whether AMPK activation affects *Gli1* mRNA levels in addition to reducing Gli1 protein stability. In $AMPK^{-/-}$ cells, *Gli1*

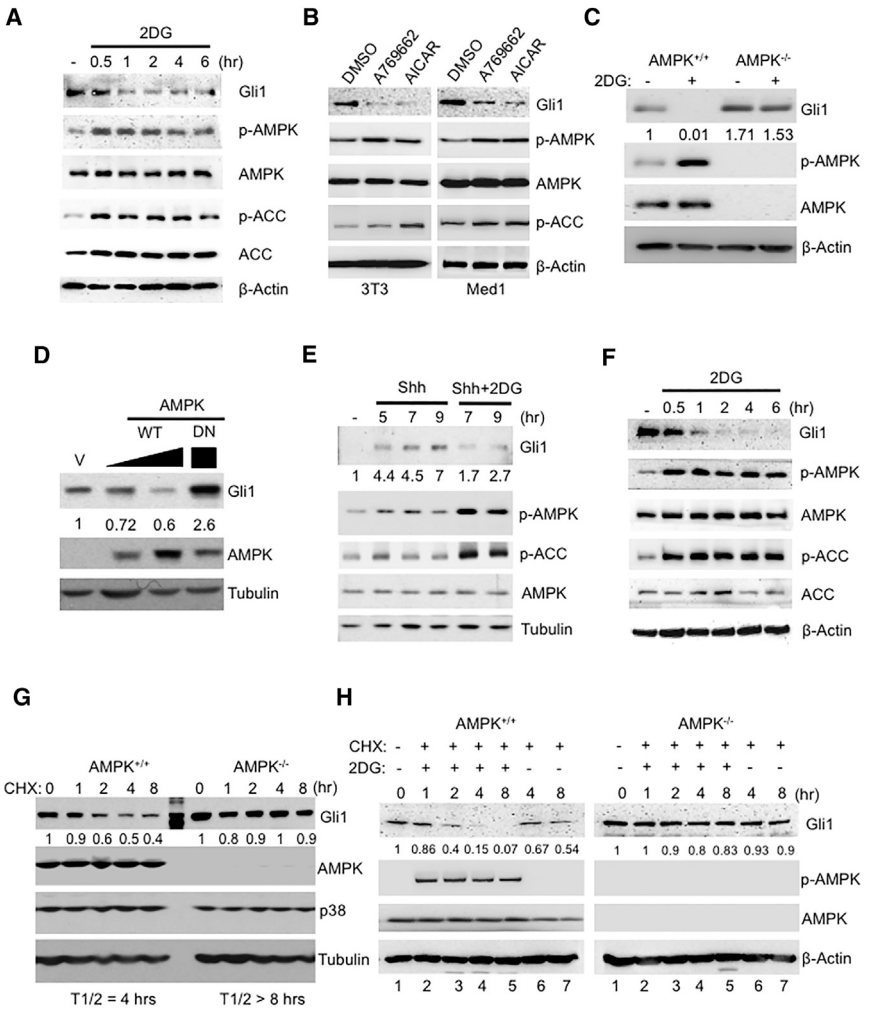

Figure 1. AMPK Reduces GLI1 Protein Levels and Stability

(A) NIH 3T3 cells were treated with 25 mM 2-deoxyglucose (2DG) for the number of hours indicated to activate AMPK. Cell lysates were analyzed via immunoblot with the indicated antibodies.

(B) NIH 3T3 and pZp53Med1 (Med1) cells were treated with 150 μM A769662 and 0.75 mM AICAR for 6 hr to activate AMPK. Cell lysates were analyzed as shown in (A).

(C) WT (*AMPK*$^{+/+}$) and KO (*AMPK*$^{-/-}$) MEF cells were treated with or without 2DG for 4 hr and lysed and analyzed as shown in (A). The Gli1 lanes were quantitated using ImageJ to determine the relative intensity to the control band, and were normalized to the internal loading control, β-actin, giving the ratio of 1.98 to 1 as indicated.

(D) HEK293 cells were transfected with genes encoding the wild-type (WT) and kinase-dead mutant (DN) forms of AMPK. Cell lysates were analyzed by immunoblot.

(E) NIH 3T3 cells were serum starved (SS) in DMEM (0.5% bovine calf serum [BCS]) overnight, stimulated with Hh for the indicated hours, and treated with 2DG (25 mM) for the number of hours indicated; lysates were analyzed by immunoblot. The western blot was measured using ImageJ to determine the relative intensities of the Gli1 bands, which were normalized using the internal loading control tubulin protein; the numbers are shown.

(F) Med1 cells, which have constitutively active Hh target gene expression, were treated with 25 mM 2DG for the indicated numbers of hours to activate AMPK. Cell lysates were analyzed by immunoblotting with the indicated antibodies.

(G) *AMPK*$^{+/+}$ and *AMPK*$^{-/-}$ MEFs were treated with cycloheximide (CHX, 1 μg ml^{-1}) for the indicated times, and cell lysates were analyzed by immunoblot with the indicated antibodies.

(H) *AMPK*$^{+/+}$ and *AMPK*$^{-/-}$ MEFs were co-treated with CHX (1 μg ml^{-1}) and with or without 2DG (25 mM) for the indicated times, and cell lysates were analyzed by immunoblot with the indicated antibodies.

and *Ptch1* mRNA were elevated about 2-fold compared to AMPK$^{+/+}$, and, consistently, mRNA from the two target genes was higher in DN-AMPK-transfected cells compared to WT-AMPK-transfected cells (Figures S2A and S2B). In NIH 3T3 cells, treatment with 2DG, A769662, and AICAR led to a time-dependent reduction in the level of mRNA from *Gli1* and from another target, *Ptch1* (Figures 2A–2C). During the 4-hr time period of examination in these experiments, the activation of AMPK by 2DG, A769662, or AICAR shut down translation and transcription, but the effect was not a general effect on mRNA levels because the control mRNA measured (*Gapdh*) did not change in amount (Figures 2A–2C). Instead, the reduced Gli1 protein, due to its instability and lowered synthesis, caused lower levels of *Gli1* and *Ptch1* transcripts. In AMPK$^{-/-}$ cells, *Gli1* mRNA remained at the same level in the presence of AICAR (Figure 2D). This result is consistent with the results shown in Figure S2A. Gli1 protein level was not affected in the presence of 2DG in AMPK$^{-/-}$ cells. In keeping with this, the addition of AMPK activators together with Shh lowered *Gli1* and *Ptch1* mRNA levels compared to induction of those targets with Shh alone (Figures 2E and S2C).

In addition to our in vitro studies with cell lines, we examined whether AMPK controls *gli1* mRNA in an in vivo context. In zebrafish embryos, treatment with 2DG led to AMPK activation and inhibition of the activity of its downstream substrate (p-ACC) (Figure S2D). Measuring *gli1* and *ptch1* mRNA levels, we found a reduction in expression levels of these genes in the 2DG-treated group compared with the untreated group (Figure S2E). Injection of ampk morpholino (MO) into zebrafish embryos led to a reduction of ampk mRNA level in comparison with the control MO (5 bp mismatches of the ampk MO) (Li et al., 2013) and 2-fold elevation of *gli1* and *ptch1* mRNA levels compared to the control group (Figure S2F).

AMPK may be acting on *Gli1* mRNA levels directly or indirectly, so we used a reporter gene assay to look at direct target gene regulation. We used a synthetic target gene consisting of eight

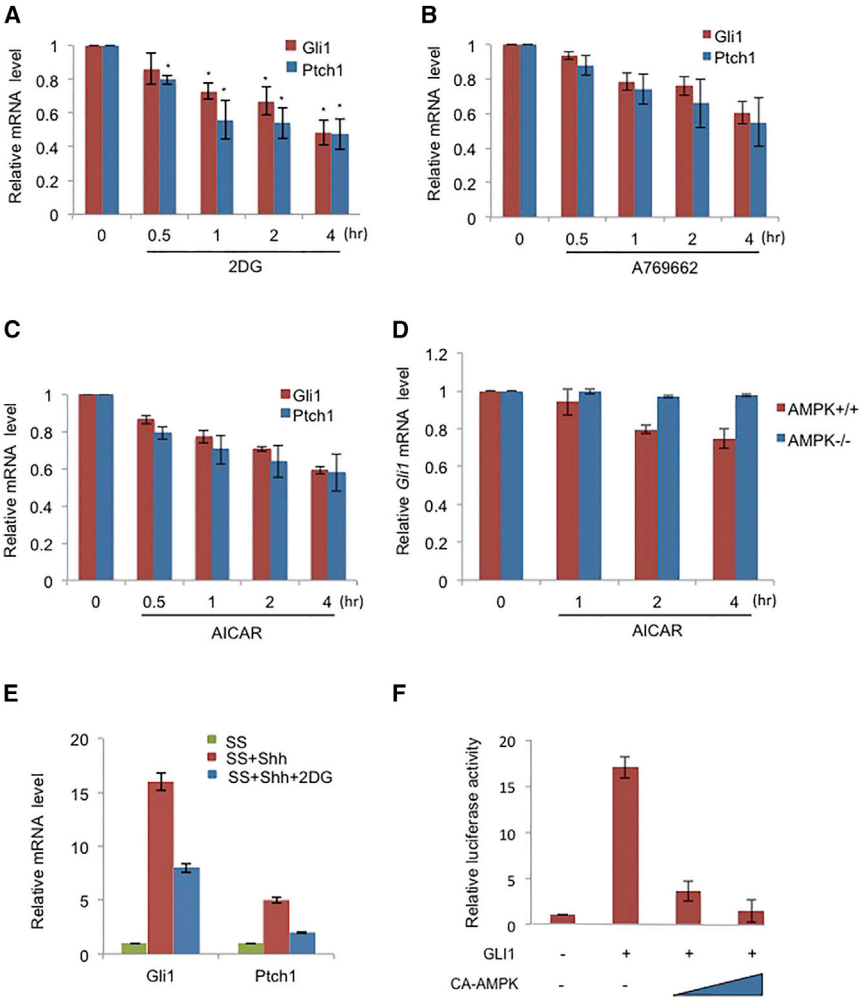

Figure 2. AMPK Inhibits GLI1 Transcriptional Activity

(A–C) NIH 3T3 cells were treated with (A) 25 mM 2DG, (B) 150 μM A769662, and (C) 0.75 mM AICAR for the indicated hours, and the amount of *Gli1* or *Ptch1* mRNA was analyzed by RT-qPCR with *Gapdh* mRNA as the internal control and normalized to the time zero *Gli1* and *Ptch1* mRNA levels. The control is provided by time zero, when no chemicals were applied, so the bars indicate *Gli1* and *Ptch1* mRNA levels relative to those of *Gapdh* and normalized to levels at time zero.

(D) $AMPK^{+/+}$ and $AMPK^{-/-}$ MEFs were treated with 0.75 mM AICAR for the indicated hours and analyzed by RT-qPCR as shown as (A).

(E) NIH 3T3 cells were SS in DMEM (0.5% BCS) overnight, stimulated with Shh with or without 25 mM 2DG for 6 hr, and the amount of *Gli1* or *Ptch1* RNA was analyzed by RT-qPCR and normalized to *Gli1* and *Ptch1* mRNA levels in SS cells. Three replicate experiments were done with SDs.

(F) HEK293 cells were co-transfected with Gli1-RE-Luciferase reporter, *GLI1*, and constitutively active *AMPK* (*CA-AMPK*), and maintained for 36 hr. Cell lysates were analyzed using a luciferase assay to measure reporter-gene transcriptional regulation by GLI1. Representative results from three experiments (n = 3) conducted in duplicate are shown with SDs.

Gli-binding sites joined to a luciferase reporter (Sasaki et al., 1997; Figure 2F). Transfection of HEK293 cells with the reporter transgene, and another plasmid that encoded constitutively active AMPK, suppressed induction by Gli1. As we show in the following experiments, target gene expression is lower because activated AMPK phosphorylates and destabilizes Gli1 protein, not because AMPK directly reduces *Gli1* mRNA.

Direct Regulation of Gli1 Protein Stability by AMPK

We next examined the mechanism of the influence of AMPK on Gli1 protein stability. To investigate whether AMPK alters Gli1 phosphorylation, we used a chemical genetic approach. The method allows specific labeling of direct substrates of a protein kinase in living cells, thus distinguishing direct from indirect influences of a kinase (Alaimo et al., 2001). ATP-binding pockets of protein kinases contain a conserved gatekeeper residue that, during the reaction, is in close contact with the N6 position of the adenine ring of ATP. Substituting a smaller amino acid for this gatekeeper residue enables the mutant protein kinase, which is termed analog specific (AS), to use ATP analogs containing bulky groups at the N6 position (Allen et al., 2007). In contrast, bulky ATP analogs are poor substrates for WT kinases due to steric hindrance by the gatekeeper residue. N6-modified ATPgS nucleotides are accepted by the AS kinase, and the transferred thiophosphate can be alkylated and recognized by a specific monoclonal antibody, thioP antibody (Allen et al., 2005, 2007). The power of the approach is exemplified by an AS version of AMPKα2 (AS-AMPKα2) that was used to identify AMPK substrates in HEK293T cells (Banko et al., 2011).

Using the same protocol, we co-transfected genes encoding HA-tagged WT or AS-AMPKα2 with the two other AMPK subunits β1 and γ1, as well as with genes for Flag-tagged GLI1 and FOXO3a into HEK293 cells. Flag antibody was used to immunoprecipitate GLI1 and FOXO3a proteins. FOXO3 is the AMPK target that served as a positive control. The precipitate was analyzed by immunoblotting with thioP antibody to detect phosphorylated GLI1 and FOXO3a. In AS-AMPKα2-transfected cells treated with 2DG, we found increased phosphorylated GLI1 compared with WT-AMPKα2-transfected cells, as well as increased phosphorylated FOXO3a (Figure 3A).

In the next experiment, we used AMPK phospho-substrate-specific antibody (p-Sub/AMPK) (Gwinn et al., 2008), and we found that Gli1 was phosphorylated in AMPK-transfected cells. HEK293 cells were transfected with Flag-tagged Gli1 alone (–) or with AMPK as well (+). Flag-tagged GLI1 was immunoprecipitated with anti-Flag antibodies and separated on a protein gel. The blot was probed with antibodies against AMPK phospho-substrate (p-Sub/AMPK), Flag, AMPK, and tubulin (Figure 3B).

The results show that GLI1-Flag was at comparable levels in both extracts, while AMPK was detected only in *AMPK*-transfected cells; a prominent band was observed with the p-Sub antibody only in cells that had been transfected with AMPK.

We generated MEFs with stable *GLI1-Flag* expression in $AMPK^{+/+}$ and $AMPK^{-/-}$ cells to verify that phosphorylation of GLI1 is AMPK dependent. AMPK was activated using 2DG and AICAR, and Flag-tagged GLI1 was immunoprecipitated with anti-Flag from $AMPK^{+/+}$ and $AMPK^{-/-}$ cell lines. In the immunoprecipitates, a prominent band was observed with the p-Sub/AMPK antibody in $AMPK^{+/+}$ MEFs, but not in $AMPK^{-/-}$ MEFs (Figure 3C). These results confirm the identity of the AMPK-phosphorylated protein as GLI1.

To discover which GLI1 amino acids were phosphorylated by AMPK, HEK293 cells were co-transfected with either WT-AMPK or DN-AMPK, and GLI1. GLI1 was purified from cell extracts using immunoprecipitation with Flag antibody, and further purified by isolating the GLI1 protein from an SDS gel. Mass spectrometry showed that GLI1 was phosphorylated at sites S102, S408, and T1074 (Figures 3D and S3). The same result was obtained in cells transfected with WT-AMPK, but not if the cells were transfected with DN-AMPK. Fourteen potential phosphopeptides were observed after two independent WT-AMPK transfections (Figures S3B–S3D, yellow). Three of these peptides were not phosphorylated in DN-AMPK-transfected cells (Figures S3B–S3D, red circles). In parallel, GLI1 was purified from stable *GLI1-Flag* expression $AMPK^{+/+}$ MEFs treated with and without 2DG to modulate endogenous AMPK activity. The same result was found that GLI1 was phosphorylated at sites S102, S408, and T1074 in 2DG-treated $AMPK^{+/+}$ MEFs (Figure S3E). Without 2DG, phosphorylations of S102 and S408 were not detected on GLI1 (Figure S3F). The results indicate that the phosphorylation changes of these sites are in response to metabolic stress in cells.

The sequence for S408 matches the AMPK consensus LRRVXS/TXXXL, but is not conserved in mouse and zebrafish. S102 and T1074 are conserved in the GLI1 proteins of humans, mice, and zebrafish (Figure 3E), but do not perfectly match the optimal AMPK consensus motif (Table S1).

The three AMPK-phosphorylated amino acids in GLI1 were changed to alanines by mutating the *Gli1* gene, i.e., S102A, S408A, and T1074A. This protein, $GLI1^{3A}$, should be immune to AMPK phosphorylation. HEK293 cells were co-transfected with DNA that encoded either WT-AMPKα2 or AS-AMPKα2, and a construct encoding $GLI1^{WT}$ or $GLI1^{3A}$ tagged with a Flag epitope. AS-AMPKα2 no longer phosphorylated the Flag-$GLI1^{3A}$ protein (Figure 3F), with the signal dropping to the background levels (0.8 arbitrary units) seen in cells transfected with WT *GLI1* (2.69 arbitrary units).

An anti-phospho-GLI1 T1074 antibody was prepared that is highly specific. Immunoprecipitated WT GLI1-Flag was stained with the p-$GLI1^{1074}$ antibody (Figure 3G, top middle lane), while the $GLI1^{3A}$ mutant (Figure 3G, top right lane) was much less so. The activation of AMPK was demonstrated here by the phospho-AMPK antibody and by the appearance of p-ACC. In this experiment, 2DG was administered for only 30 min, sufficient to activate AMPK, but not long enough to cause loss of GLI1 protein (Figures 1A and 1F). 2DG was necessary for substantial labeling of the WT protein (Figure 3G, top middle lane compared to top left lane). The 2DG-driven phosphorylation of GLI1 was observed with cells transfected with WT *GLI1*, but not with cells transfected with $GLI1^{3A}$ mutant (Figures 3G and S3G). To identify which AMPK phosphorylation site predominates, we repeated the experiment of Figure 2B and co-transfected $GLI1^{WT}$, $GLI1^{3A}$, the three single mutants, and $GLI1^{102A/1074A}$ with AMPK into HEK293 cells. In cells transfected with $GLI1^{3A}$, no signal was detected with p-Sub/AMPK, and in cells containing $GLI1^{408A}$, the signal had 28% of the intensity compared with $GLI1^{WT}$ (Figure 3H). $GLI1^{102A}$ and $GLI1^{1074A}$ had 57% and 42% of the control signal, respectively, and the signal of the 102A/1074A double mutant was lower at 35% of the control (Figure 3H).

To prove that AMPK can act directly upon GLI1, an in vitro AMPK assay was performed. In Figure 3I, $GLI1^{3A}$ was utterly resistant to AMPK, which is similar to results shown in Figure 3H. Each single mutation (102A, 408A, and 1074A) moderately reduced the modification by AMPK, from 20% to 60% (Figure 3I). We conclude that S102, S408, and T1074 are all dominant AMPK phosphorylation sites on GLI1.

$GLI1^{3A}$ Has Higher Protein Stability and Transcriptional Activity

Here we show that, compared to $GLI1^{WT}$, the $GLI1^{3A}$ mutant protein has increased stability, is resistant to AMPK-mediated suppression of Gli1 transcriptional activity, and stabilizes *Gli1* mRNA at high levels. Using CHX to prevent new protein synthesis as in Figure 1, we found that, in transfected HEK293 cells, $GLI1^{3A}$ is considerably more stable than $GLI1^{WT}$. We produced a phospho-mimic version of GLI1 where each of the three AMPK-phosphorylated residues was replaced by a glutamate; this was called $GLI1^{3E}$ and was highly unstable (Figure 4A, right). Similarly, $GLI1^{3A}$ was much more stable than $GLI1^{3E}$ or $GLI1^{WT}$ in NIH 3T3 cell lines in which GLI1 was stably produced (Figure S4A).

To examine regulation of transcription by each version of GLI1, we transfected genes encoding each of the forms into HEK293 cells. Each variant GLI1 was tested with or without co-transfected AMPK. Activation of transcription by *GLI1* was measured with a luciferase assay; the cells also were transfected with a plasmid encoding eight Gli consensus sequences in *cis* to a luciferase gene (Sasaki et al., 1997). Transfected *GLI1* activated this target even without added Shh or other agonists. The samples were normalized by comparison to cells transfected with vector alone. Transcriptional induction by WT GLI1 was negatively affected by adding AMPK, produced at two levels by transfecting 1 or 3 μg, even without adding 2DG (Figure 4B). In contrast, $GLI1^{3A}$ transcriptional activity was refractory to inhibition by AMPK even at the higher level (Figure 4C). Further activation of AMPK by added 2DG inhibited GLI1 target gene expression if cells contained $GLI1^{WT}$, but not if cells contained $GLI1^{3A}$ (Figures 4D and 4E). We repeated the experiments using other AMPK activators (AICAR and A79662) (Banko et al., 2011) in NIH 3T3 cell lines stably expressing GLI1 proteins. $GLI1^{3A}$ had robust resistance to 2DG-induced lowering of *Gli1*/*Ptch1* mRNA levels (Figures 4F and 4G). Each single mutant had a different degree of moderate to great resistance to 2DG effects (Figures S4B

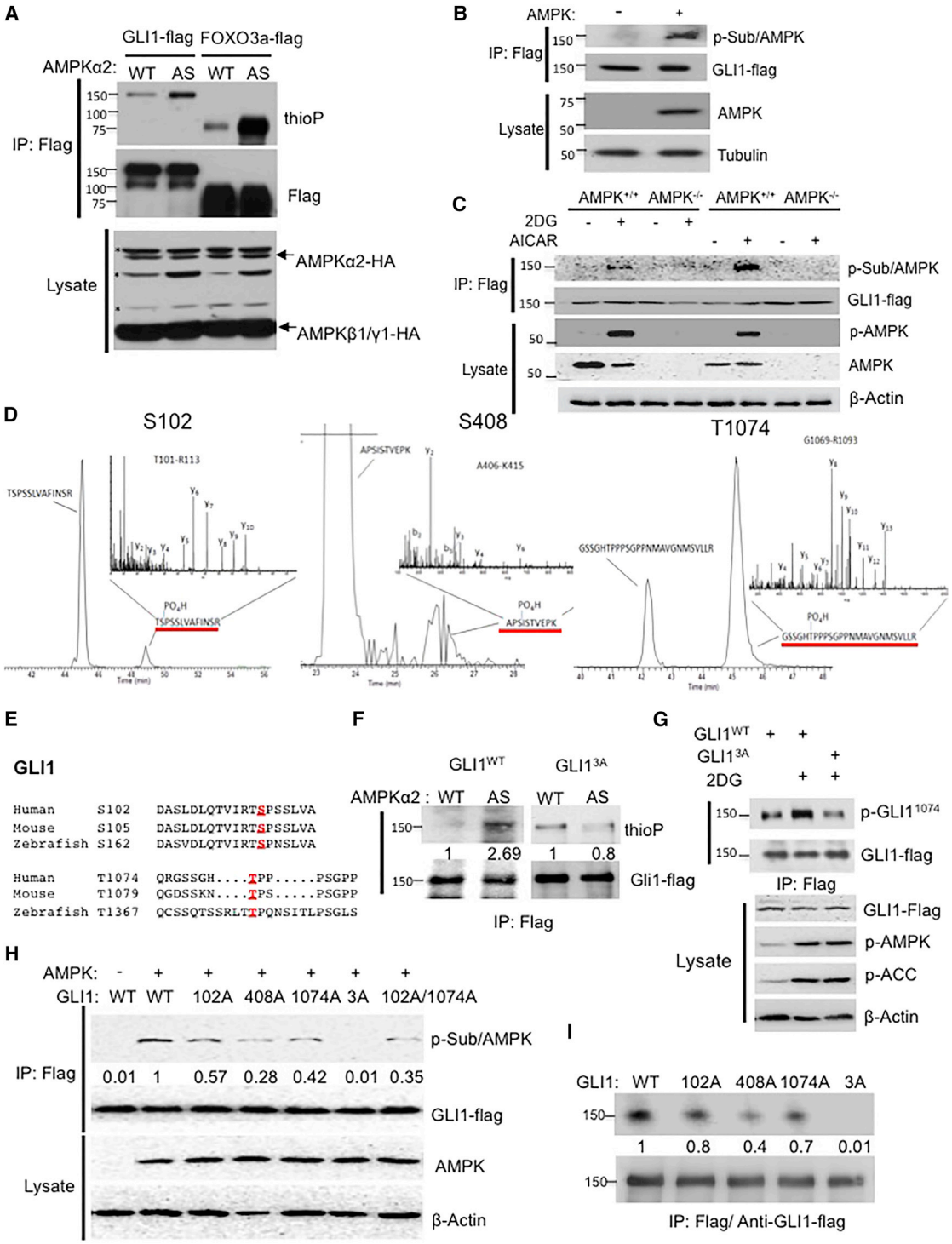

Figure 3. AMPK Directly Phosphorylates GLI1

(A) HEK293 cells were co-transfected with Flag-tagged GLI1 or Flag-tagged FOXO3, with HA-tagged WT or AS-AMPKα2, and with AMPKβ1 and γ1. AS-AMPKα2 phosphorylates the known AMPK substrate FOXO3, which was detected using thioP antibody. FOXO3 and GLI1 were immunoprecipitated with antibodies that recognize the Flag tag and blotted with thioP, Flag, or HA (AMPK) antibody. *Non-specific bands that were recognized by HA antibody.

(B) HEK293 cells were co-transfected with Flag-tagged GLI1 and HA-tagged AMPK, and cells were lysed in NP40 lysis buffer. GLI1 was immunoprecipitated using an antibody to Flag and the precipitate was analyzed on a protein blot using AMPK phosphorylation-specific substrate antibody (p-Sub/AMPK) and Flag antibody. The introduction of AMPK into the cells causes p-Sub/AMPK to label GLI1-Flag.

(legend continued on next page)

and S4C). These results indicate that mutation of the three residues to alanine did indeed make GLI1 function refractory to inhibition by AMPK.

GLI1^{3A} Has Potent Cell Division-Stimulating and Oncogenic Activity

To further investigate the function of these GLI1 mutants, we generated stable cell lines in NIH 3T3 cells using lentiviral vectors that produced GLI1^{WT}, GLI1^{3A}, or GLI1^{3E}. The amount of GLI1^{3A} protein that accumulated was about 1.4-fold that seen for GLI1^{WT}, normalizing both to actin (Figure 5A). Cell counting with a hemacytometer showed that cells transduced with *GLI1^{3A}* virus had a significantly increased growth rate compared to WT and GLI1^{3E} cell lines (Figure 5B). Colony formation assays (Figure 5C) showed increased growth of GLI1^{3A}-bearing mutant cells compared to other cell lines. To test the effect of activating AMPK, 25 mM 2DG was added to the starting cultures and the growth of colonies was measured 2 weeks later. An even higher colony number difference was observed after treatment with 2DG (Figure 5D; Yang et al., 2008), but only for cells containing GLI1^{3A}. Similar results were obtained using A769662 and AICAR in the colony formation assay (Figure S5). To test the oncogenic impact of GLI1^{WT} in comparison to the mutant proteins, the stably transfected cell lines producing the GLI1 variants were injected subcutaneously into nude mice. Tumor growth was monitored for 3 weeks. Cells that contained GLI1^{3A} grew to a volume about 2.5 times that of the other three cell lines (Figure 5E).

DISCUSSION

The Hh pathway controls cell differentiation and growth in developing embryos and regenerating adult tissues. Most features of the pathway components and their interactions are evolutionarily conserved across many species from *Drosophila* to humans, in developing and adult animals experiencing deprivation and stresses, as well as circadian and annual rhythms that demand adaptation of developmental mechanisms to circumstances. One way that this happens is that the pathway itself has built-in feedback controls that buffer the signaling. For example, induction of the *Gli1* gene by the pathway creates a positive feedback loop that can maintain expression of target genes including *Gli1* itself. A restraining effect is mediated by the induction of *ptch* by the pathway, since the Ptch protein is a negative regulator. The amount of Ptch increases in response to increased Hh ligand, so the pathway is buffered. Too much ligand may be reined in by extra Ptch antagonist.

While these sorts of feedback controls are important, they do not cope with the need to coordinate with all relevant aspects of physiology. In particular, dramatic changes in energy stores occur due to the changing abundance of food. Elaborate mechanisms have evolved for cells to adapt to high or low levels of ATP (Hardie et al., 2012; Inoki et al., 2012). In some tissues, such as fly wing discs and mammalian cerebellum, Hh signaling has powerful growth effects. Embarking on that growth when ATP is scarce is unlikely to succeed and may lead to fatal imbalances among tissues and cell types. Thus, activation of AMPK in response to high AMP levels shuts down central processes, such as protein synthesis and ion transport (Lang and Föller, 2014), while boosting other processes that increase hardiness and allow survival until ATP stores are rebuilt. AMPK has many target proteins that, together, allow coordinated shutdown of energy-demanding activities (Hardie et al., 2012). Its activity can be triggered by stimuli such as exercise (Jessen et al., 2014), cytokines, and hypoxia (Evans et al., 2012). Targets have been identified in several ways, such as whole-cell proteomics (Banko et al., 2011), in vitro tests (Gwinn et al., 2008), and genetics (Mihaylova and Shaw, 2011). The full range of targets is not known, but among them are transcription factors such as E2F1 (Yang et al., 2014), Msn2 (Petrenko et al., 2013), and FoxO3a (Greer et al., 2007). A recent paper showed that AMPK negatively regulates Gli1 in hepatocellular carcinoma (HCC), but did not address the mechanism (Abi et al., 2011; Xu et al., 2014). They showed that expression of AMPK is negatively correlated with Gli1 in HCC. Their work provides a useful example of the effect of reduced AMPK function in a tumor; as in our experiments, tumor growth is stimulated when Gli1 is not targeted by AMPK.

(C) *AMPK$^{+/+}$* and *AMPK$^{-/-}$* MEFs were virus infected with Flag-tagged GLI1 and treated with 25 mM 2DG and 0.75 mM AICAR for 30 min, and cells were lysed in NP40 lysis buffer. The cells lysates were analyzed as shown as (B).

(D) HEK293 cells were co-transfected with Flag-tagged GLI1 and AMPKα2, β1, and γ1. Cells were lysed in NP40 lysis buffer. The lysates were subjected to immunoprecipitation using an antibody to Flag-tag, and the GLI1 band was isolated and subjected to mass spectrometry. Extracted ion chromatograms (EICs) identified phosphorylated peptides S102, S408, and T1074. The insets represent the fragment ion spectra determined using high-energy dissociation (HCD).

(E) Alignment of two conserved sites (S102 and T1074) in GLI1 that match the optimal AMPK substrate motif and are conserved from human to zebrafish. S408 is present only in the human sequence.

(F) HEK293 cells were co-transfected with Flag-tagged GLI1^{WT} or Flag-tagged GLI1^{3A}, either WT-AMPKα2 or AS-AMPKα2, and AMPK β1 and γ1. Cells were lysed in NP40 lysis buffer. Substrates were immunoprecipitated with antibodies to Flag-M2 and blotted with thioP or Flag antibody.

(G) 2DG-stimulated phosphorylation of GLI1. (Left) HEK293 cells were transfected with Flag-tagged GLI1^{WT} or GLI1^{3A}; 36 hr after transfection, they were treated with 25 mM 2DG for 30 min, long enough to activate AMPK but not long enough to cause breakdown of Gli1. The lysates were subjected to immunoprecipitation using an antibody to Flag-tag and immunoblotted with phospho-GLI1^{1074} and Flag antibodies. The strong labeling in the center top lane shows that WT GLI1, but not GLI1^{3A}, is phosphorylated by AMPK. (Right) Lysates prepared as at left were immunoblotted with antibodies against Flag, phospho-AMPK (p-AMPK), phospho-ACC (p-ACC), and β-actin. The p-AMPK and p-ACC lanes show that the AMPK is stimulated by the 2DG. The actin lane controls for loading. The GLI1-Flag lane shows stabilization of GLI1^{wt} and of GLI1^{3A} in response to 2DG, though the response to 2DG disappears by 30 min.

(H) HEK293 cells were transfected with AMPK and Flag-tagged GLI1^{WT}, GLI1^{102A}, GLI1^{408A}, GLI1^{1074A}, GLI1$^{102A/1074A}$, and GLI1^{3A}. Gli1 was immunoprecipitated using an antibody to Flag and the precipitate was analyzed on a protein blot using AMPK phosphorylation-specific substrate antibody (p-Sub/AMPK) and Flag antibody. The introduction of AMPK into the cells causes p-Sub/AMPK to label GLI1-Flag. The number indicates the relative intensity of p-Sub/AMPK antibody.

(I) HEK293 cells were transfected with Flag-tagged GLI1^{WT}, GLI1^{102A}, GLI1^{408A}, GLI1^{1074A}, and GLI1^{3A}. Cells were lysed in NP40 lysis buffer. Cell lysates were immunoprecipitated with antibodies to Flag-M2 and the immunoprecipitated GLI1 proteins were subjected to in vitro AMPK assay. The number indicates the relative intensity of AMPK activity.

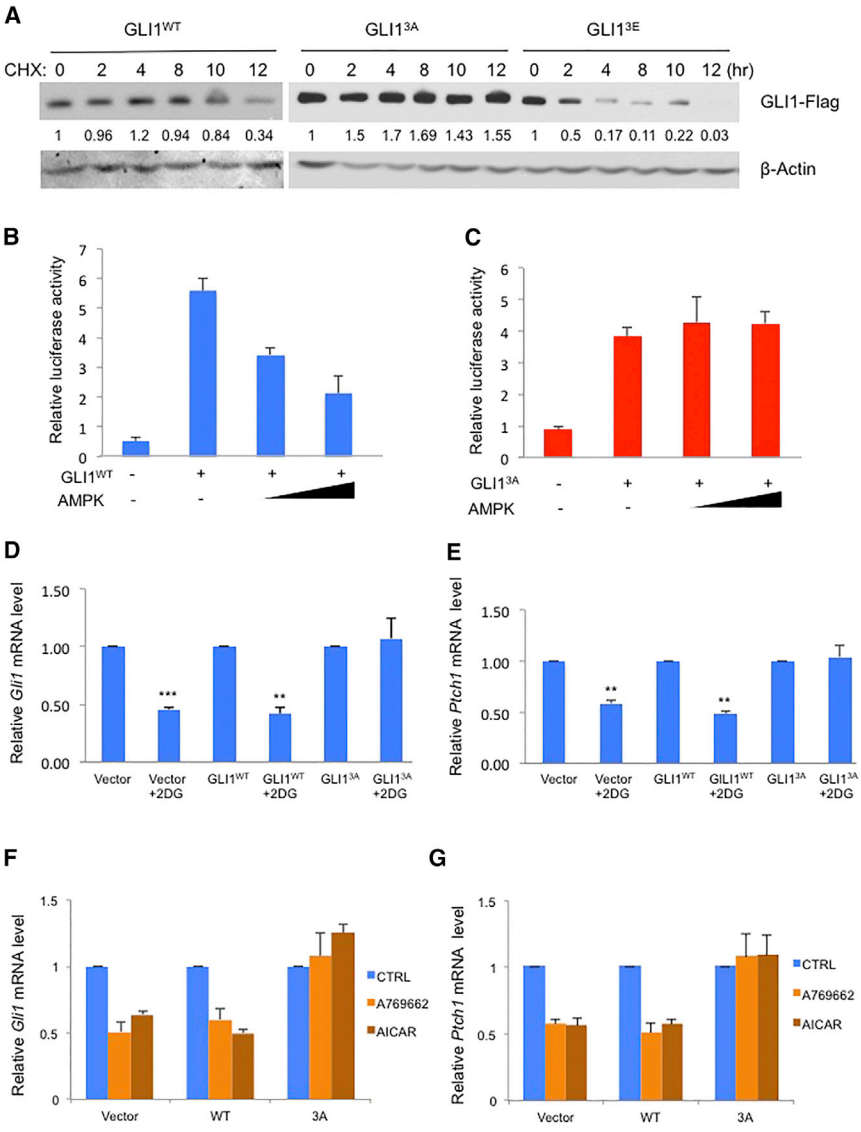

Figure 4. GLI1^{3A} Has Higher Protein Stability and Transcriptional Activity

The GLI1^{3A} mutant has increased stability and is resistant to AMPK-mediated suppression of Gli1 transcriptional activity.

(A) Lysates of HEK293 cells transfected with Flag-*GLI1*^{WT}, Flag-*GLI1*^{3A}, or Flag-*GLI1*^{3E} were harvested at different times after treatment with CHX (1 μg ml^{-1}) and analyzed by immunoblot. GLI1^{3E} has the two serines and one threonine that are normally phosphorylated by AMPK changed into glutamates to mimic phosphorylated GLI1.

(B) HEK293 cells were co-transfected with Gli1-luciferase reporter, *Gli1*^{WT}, and *AMPK* for 36 hr. The two amounts of AMPK-expressing plasmid used were 1 and 3 μg. Cell lysates were analyzed using a luciferase assay to measure GLI1 transcriptional induction of the introduced Gli1-luciferase target gene. Representative results from three experiments (n = 3), each conducted in duplicate, are shown with SDs.

(C) HEK293 cells were co-transfected with Gli1-luciferase reporter, *GLI1*^{3A}, and *AMPK* and analyzed as in (B).

(D and E) NIH 3T3 cells were transfected with vector control, *GLI1*^{WT}, or *GLI1*^{3A} for 36 hr, then treated with 2DG (25 mM) for 4 hr. RT-PCR was used to measure (D) *Gli1* mRNA and (E) *Ptch1* mRNA. The experiment was repeated three times (**$p < 0.01$, ***$p < 0.001$).

(F and G) NIH 3T3 vector, GLI1^{WT}, and GLI1^{3A} producing stable cell lines were treated with AICAR (0.75 mM) and A769662 (150 μM) for 4 hr. RT-PCR was used to measure (F) *Gli1* mRNA and (G) *Ptch1* mRNA. The experiment was repeated three times.

Our research shows that GLI1 can be added to the list of direct AMPK targets. S408 is found in a sequence that perfectly matches the AMPK consensus site, while S102 and T1074 (SP and TP) sequences are not perfectly matched to the traditional AMPK consensus site. We examined other kinases such as p38 and JNK, MAPK-type proline-directed kinases, and found that their inhibition did not influence Gli1 protein levels (data not shown). Mutation of each of the individual sites on Gli1 impacts AMPK-mediated phosphorylation activity, and each mutation site may exert effects on other sites (Figures 3H and S3G). Overall, current results show that two sets of AMPK-dependent phosphorylation sites include two SP/TP sites (S102 and T1074, Figures S3E and S3F), with high basal stoichiometry and modest inducibility, and one site matching the AMPK consensus (S408, Figures S3E and S3F), with low basal stoichiometry but very high inducibility. Collectively, these AMPK-regulated sites in GLI1 control its protein stability.

Post-translational modification of Gli proteins by other signaling pathways contributes to the formation of many cancers with elevated Gli activity (Amakye et al., 2013; Hui and Angers, 2011; Niewiadomski et al., 2014). The mTOR/S6K kinase pathway was shown to enhance Gli1 transcriptional activity (Wang et al., 2012). Since the mTOR/S6K pathway has been reported to be involved in the development of various tumors, targeting mTOR is becoming one of the major methods for cancer treatment. In addition, AMPK has been shown to suppress mTOR/S6K1 activity through direct phosphorylation of mTOR and Tuberous Sclerosis Complex (Kim et al., 2008), the upstream negative regulator of mTOR (Kahn et al., 2005). Given our findings, we now know that AMPK both directly and indirectly suppresses the Hh/Gli1 pathway. AMPK conditional knockout models have been created (Viollet et al., 2009), but the role of AMPK in tumorigenesis has not been extensively studied. Loss of AMPK is insufficient to provoke tumor formation in mice, but genetic ablation of the α1 catalytic subunit of AMPK accelerates the development of lymphomas driven by *Myc* overexpression (Faubert et al., 2013). In contrast, deletion of the AMPKα2, but not the AMPKα1, subunit of AMPK increases susceptibility to H-RasV12-induced

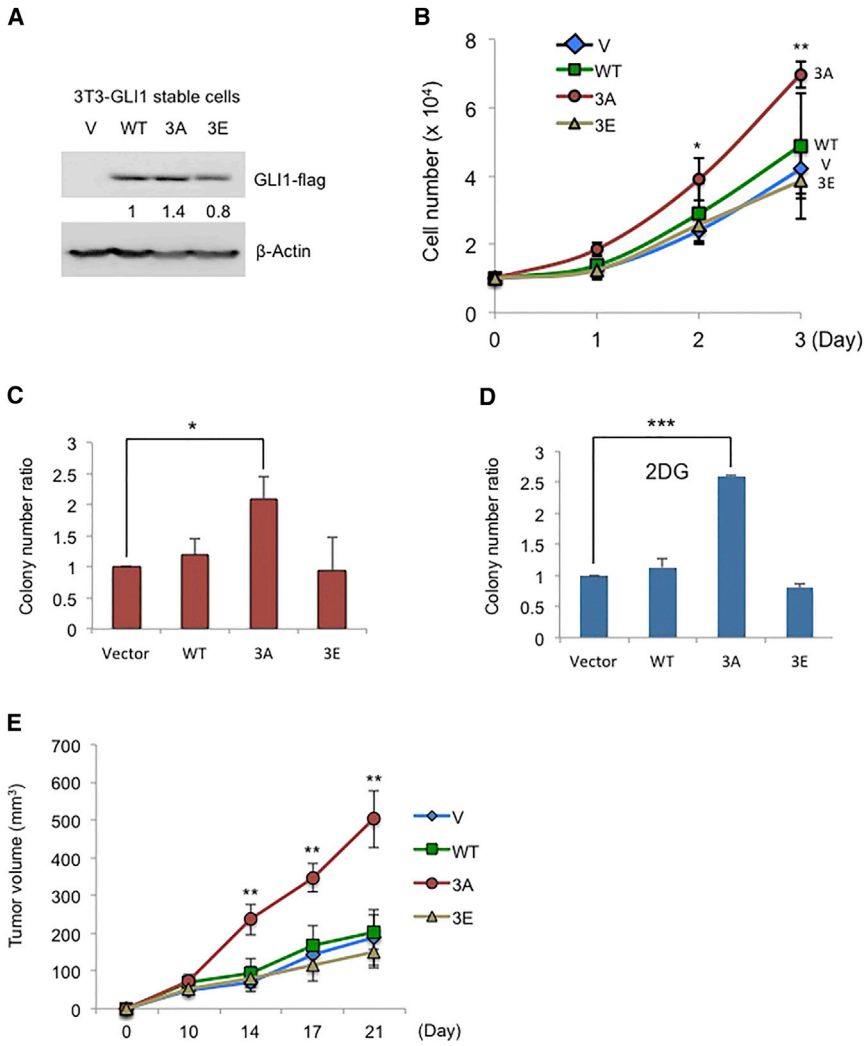

Figure 5. Tests of Cell Division, Colony Formation, and Oncogenic Effects of Mutant GLI1 Proteins

(A) NIH 3T3 cells were infected with vector, $GLI1^{WT}$, $GLI1^{3A}$, or $GLI1^{3E}$ lentivirus, with Flag tags on each protein, and selected for 7 days with puromycin (2.5 $\mu g/ml^{-1}$). Cell lysates were analyzed by immunoblotting with Flag antibody to measure the amounts of the expressed proteins.

(B) This experiment used NIH 3T3 GLI1-stable cell lines (vector control, WT, 3A, and 3E). 5×10^3 cells were seeded into 12-well plates for growth assays, each cell type in triplicate, and cells were counted using a hemocytometer for 3 consecutive days. The experiment was repeated three times (*$p < 0.01$, **$p < 0.001$).

(C) NIH 3T3 cells with $GLI1^{WT}$, $GLI1^{3A}$, or $GLI1^{3E}$ stably expressed were seeded into six-well plates for colony formation assays for 2 weeks. Colonies larger than 1.5 mm were counted.

(D) As in (C), the cells were treated with 2DG (25 mM) and 2DG-containing medium. The medium in 2DG-treated wells was changed every 3 days to refresh the 2DG. Colony numbers were counted 2 weeks later. In (C) and (D), each cell line was seeded in duplicate, with n = 3 (*$p < 0.05$, ***$p < 0.0001$).

(E) NIH 3T3 GLI1-stable cell lines (vector control, WT, 3A, and 3E). 10^7 cells were injected subcutaneously into the nude mice and tumor growth was monitored for 3 weeks (**$p < 0.001$).

transformation in murine fibroblasts (Phoenix et al., 2012), raising the interesting possibility that the AMPKα2 subunit may contribute to tumor suppression in a way that is independent of, or in addition to, the energy-sensing function of AMPK. This suggests that AMPK activity opposes tumorigenesis. Loss of AMPK function evidently fosters tumor progression, perhaps by heightening activities of pathways that spur cell growth and proliferation.

In summary, we found that AMPK inhibits Gli1 protein levels and transcriptional activity. AMPK phosphorylated GLI1 at three novel sites and induced GLI1 protein degradation. Mutation of these three sites into alanine prolonged GLI1 protein stability, transcriptional activity, and oncogenic function (Figure 6). We report here that an energy sensor, AMPK, directly targets the Hh transcriptional activator, GLI1, and suppresses GLI1 activity. Revealing the detailed molecular mechanism of how AMPK modulates the Hh pathway will enable us to further understand the coordination between energy metabolism regulation and the Hh pathway during development.

EXPERIMENTAL PROCEDURES

All human subjects and animal manipulation protocol were under regulations of institutional review board (IRB 1203012078) and Purdue Animal Care and Use Committee (PACUC 1301000800), respectively.

Reagents and Plasmids

AMPK activators 2DG and metformin were purchased from Sigma, AICAR was from Calbiochem, and A-769662 was from Selleckchem. CHX and glucose were purchased from Sigma. The dual-luciferase assay kit was purchased from Promega. The Gli1-luciferase reporter contained eight directly repeated copies of the consensus Gli1-binding site (Sasaki et al., 1997). GLI1 HA-tagged, Flag-tagged, and pCDH-CMV-MCS-EF1-Puro constructs were gifts from Dr. Mien-Chie Hung (Wang et al., 2012) (University of Texas MD Anderson Cancer Center). LKB1 shRNA plasmids were gifts from Dr. Hui-Kuan Lin (University of Texas MD Anderson Cancer Center). Mutated constructs derived from the control HA-tagged and Flag-tagged $GLI1^{3A}$ and $GLI1^{3E}$ were generated using the Quick Change multisite-directed mutagenesis kit from Stratagene. NheI-forward primer (5′ GGCGAGCTAGCATGGACTACAAAGACCATGAC 3′) and BstBI-reverse primer (5′ AGTATTCGACACCCCGGATCCTC 3′) were used to subclone the $GLI1^{WT}$, $GLI1^{3A}$, and $GLI1^{3E}$ into pCDH-CMV-MCS-EF1-Puro.

Immunoblotting and Immunoprecipitation Assays

Immunoblotting and immunoprecipitation were performed as previously described (Yang et al., 2008), with the following antibodies: Gli1 and GFP (Santa Cruz Biotechnology); Gli1, AMPK, p-AMPK, ACC, p-ACC, p-AMPK/Sub, LKB1, JNK, p-JNK, p-38, and p-p38 (Cell Signaling Technology); Actin, Tubulin, Flag-M2 (Sigma), and HA (Roche); and Thiophosphate Ester Specific Ab (Epitomics). The Gli1 antibody used to generate the data shown was of the Santa Cruz Biotechnology and Cell Signaling Technology antibodies at 1:1,000 dilution in 3% milk.

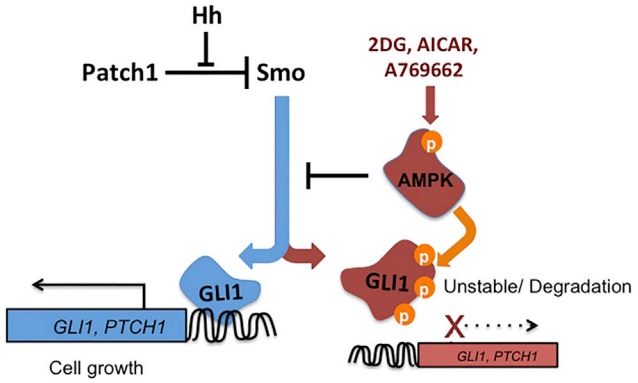

Figure 6. AMPK Phosphorylates GLI1 and Inhibits Hedgehog Pathway

The diagram shows that activated AMPK directly phosphorylates GLI1 on S102, S408, and T1074 sites. Phosphorylation lowers GLI1 protein stability, thus reducing GLI1 transcriptional activity, and mitigates cell growth.

Real-Time qPCR

Total RNA was isolated from NIH 3T3 fibroblasts and PZp53^{MED} cells using Trizol reagent (Invitrogen). RNA (1 μg) was reverse-transcribed with random hexamer primers using SuperScript III reverse transcriptase (Invitrogen). A fraction (1/20) of the resultant cDNA was used as a template for amplification with TaqMan qPCR probes (Applied Biosystems) on an Applied Biosystems 7500 Fast thermocycler as follows: Gapdh (Mm99999915_g1), Gli1 (Mm00494645_m1), and Ptc1 (Mm00436026_m1).

Cell Culture, MTT Cell Growth, and Colony Formation Assay Analysis

NIH 3T3 cells were cultured in DMEM supplemented with 10% bovine calf serum (BCS) at 5% CO_2. All other cell cultures were kept in DMEM supplemented with 10% fetal bovine serum (FBS) at 5% CO_2. The concentrations and time for each chemical treatment were as follows: 2DG (25 mM, 4 hr) and CHX (1 μg ml^{-1}), unless otherwise noted. The cell growth rate was determined using MTT and cell-counting assays (Yang et al., 2008). For colony formation assays, 5 × 10^4 cells were placed in 1.5 ml DMEM with 10% FBS and 0.3% agarose and overlaid onto 3 ml DMEM with 10% FBS and 0.6% agarose in each well of a six-well plate; medium with or without 25 mM 2DG was applied to each well until the end of the assay. After 2–3 weeks, colonies larger than 2 mm in diameter were counted.

SUPPLEMENTAL INFORMATION

Supplemental Information includes Supplemental Experimental Procedures, five figures, and one table and can be found with this article online at http://dx.doi.org/10.1016/j.celrep.2015.06.054.

AUTHOR CONTRIBUTIONS

J.-Y.Y designed, performed, and coordinated research. J.-Y.Y., Y.-H.L., J.L., Y.-Y.C.M., V.E.H., J.C., and M.R.B. performed research. J.-Y.Y. analyzed the data. All authors contributed to discussions of results and interpretations. J.L. and M.P.S wrote part of the manuscript and J.-Y.Y. wrote the paper.

ACKNOWLEDGMENTS

We thank Mien-Chie Hung (University of Texas M.D. Anderson Cancer Center) for GLI1 HA-tagged and Flag-tagged constructs; Hui-Kuan Lin (University of Texas M.D. Anderson Cancer Center) for LKB1 shRNA constructs; Keith R. Laderoute for the AMPK MEF cells (SRI International); and Xiaoqi Liu and W. Andy Tao (Purdue University) for technical support. We also thank Sherri Huang (Indiana University) and Ljiljana Milenkovic (Stanford University) for commenting on the manuscript. This work was supported by a Showalter Research Scholar grant (207655 to J.-Y.Y.); P30 CA023168 to the Purdue University Center for Cancer Research in support of the use of facilities; and American Cancer Society Institutional Research Grant 58-006-53 to the Purdue University Center for Cancer Research and Purdue Start-up Fund (J.-Y.Y.). J.-Y.Y. was partly supported by NIH Tumor Biology Training Fellowship (NIH T32CA09151) and Lucile Packard Foundation, and Stanford CTSA (UL1RR025744) when the project was initiated in M.P.S.'s lab. Y.-H.L. was supported by Postdoctoral Research Abroad Program 103-2917-I-564-036, Taiwan.

Received: March 26, 2015
Revised: May 11, 2015
Accepted: June 15, 2015
Published: July 16, 2015

REFERENCES

Abi, K.S., Haddad-Zebouni, S., Roukoz, S., Smayra, T., Kamal, H., Menassa-Moussa, L., Aoun, N.J., and Ghossain, M.A. (2011). Ultrasound as an adjunct to radiography in minor musculoskeletal pediatric trauma. J. Med. Liban. *59*, 70–74.

Alaimo, P.J., Shogren-Knaak, M.A., and Shokat, K.M. (2001). Chemical genetic approaches for the elucidation of signaling pathways. Curr. Opin. Chem. Biol. *5*, 360–367.

Allen, J.J., Lazerwith, S.E., and Shokat, K.M. (2005). Bio-orthogonal affinity purification of direct kinase substrates. J. Am. Chem. Soc. *127*, 5288–5289.

Allen, J.J., Li, M., Brinkworth, C.S., Paulson, J.L., Wang, D., Hübner, A., Chou, W.H., Davis, R.J., Burlingame, A.L., Messing, R.O., et al. (2007). A semisynthetic epitope for kinase substrates. Nat. Methods *4*, 511–516.

Amakye, D., Jagani, Z., and Dorsch, M. (2013). Unraveling the therapeutic potential of the Hedgehog pathway in cancer. Nat. Med. *19*, 1410–1422.

Banko, M.R., Allen, J.J., Schaffer, B.E., Wilker, E.W., Tsou, P., White, J.L., Villén, J., Wang, B., Kim, S.R., Sakamoto, K., et al. (2011). Chemical genetic screen for AMPKα2 substrates uncovers a network of proteins involved in mitosis. Mol. Cell *44*, 878–892.

Berman, D.M., Karhadkar, S.S., Hallahan, A.R., Pritchard, J.I., Eberhart, C.G., Watkins, D.N., Chen, J.K., Cooper, M.K., Taipale, J., Olson, J.M., and Beachy, P.A. (2002). Medulloblastoma growth inhibition by hedgehog pathway blockade. Science *297*, 1559–1561.

Evans, A.M., Peers, C., Wyatt, C.N., Kumar, P., and Hardie, D.G. (2012). Ion channel regulation by the LKB1-AMPK signalling pathway: the key to carotid body activation by hypoxia and metabolic homeostasis at the whole body level. Adv. Exp. Med. Biol. *758*, 81–90.

Faubert, B., Boily, G., Izreig, S., Griss, T., Samborska, B., Dong, Z., Dupuy, F., Chambers, C., Fuerth, B.J., Viollet, B., et al. (2013). AMPK is a negative regulator of the Warburg effect and suppresses tumor growth in vivo. Cell Metab. *17*, 113–124.

Greer, E.L., Oskoui, P.R., Banko, M.R., Maniar, J.M., Gygi, M.P., Gygi, S.P., and Brunet, A. (2007). The energy sensor AMP-activated protein kinase directly regulates the mammalian FOXO3 transcription factor. J. Biol. Chem. *282*, 30107–30119.

Gwinn, D.M., Shackelford, D.B., Egan, D.F., Mihaylova, M.M., Mery, A., Vasquez, D.S., Turk, B.E., and Shaw, R.J. (2008). AMPK phosphorylation of raptor mediates a metabolic checkpoint. Mol. Cell *30*, 214–226.

Hardie, D.G., Ross, F.A., and Hawley, S.A. (2012). AMPK: a nutrient and energy sensor that maintains energy homeostasis. Nat. Rev. Mol. Cell Biol. *13*, 251–262.

Henin, N., Vincent, M.F., Gruber, H.E., and Van den Berghe, G. (1995). Inhibition of fatty acid and cholesterol synthesis by stimulation of AMP-activated protein kinase. FASEB J. *9*, 541–546.

Hui, C.C., and Angers, S. (2011). Gli proteins in development and disease. Annu. Rev. Cell Dev. Biol. *27*, 513–537.

Inoki, K., Kim, J., and Guan, K.L. (2012). AMPK and mTOR in cellular energy homeostasis and drug targets. Annu. Rev. Pharmacol. Toxicol. *52*, 381–400.

Jacob, L.S., Wu, X., Dodge, M.E., Fan, C.W., Kulak, O., Chen, B., Tang, W., Wang, B., Amatruda, J.F., and Lum, L. (2011). Genome-wide RNAi screen reveals disease-associated genes that are common to Hedgehog and Wnt signaling. Sci. Signal. *4*, ra4.

Jessen, N., Sundelin, E.I., and Møller, A.B. (2014). AMP kinase in exercise adaptation of skeletal muscle. Drug Discov. Today *19*, 999–1002.

Jishage, K., Nezu, J., Kawase, Y., Iwata, T., Watanabe, M., Miyoshi, A., Ose, A., Habu, K., Kake, T., Kamada, N., et al. (2002). Role of Lkb1, the causative gene of Peutz-Jegher's syndrome, in embryogenesis and polyposis. Proc. Natl. Acad. Sci. USA *99*, 8903–8908.

Kahn, B.B., Alquier, T., Carling, D., and Hardie, D.G. (2005). AMP-activated protein kinase: ancient energy gauge provides clues to modern understanding of metabolism. Cell Metab. *1*, 15–25.

Kim, J.S., Romero, R., Tarca, A.L., LaJeunesse, C., Han, Y.M., Kim, M.J., Suh, Y.L., Draghici, S., Mittal, P., Gotsch, F., et al. (2008). Gene expression profiling demonstrates a novel role for foetal fibrocytes and the umbilical vessels in human fetoplacental development. J. Cell. Mol. Med. *12*, 1317–1330.

Lang, F., and Föller, M. (2014). Regulation of ion channels and transporters by AMP-activated kinase (AMPK). Channels (Austin) *8*, 20–28.

Li, Y.H., Chen, H.Y., Li, Y.W., Wu, S.Y., Wangta-Liu, Lin, G.H., Hu, S.Y., Chang, Z.K., Gong, H.Y., Liao, C.H., et al. (2013). Progranulin regulates zebrafish muscle growth and regeneration through maintaining the pool of myogenic progenitor cells. Sci. Rep. *3*, 1176.

Mihaylova, M.M., and Shaw, R.J. (2011). The AMPK signalling pathway coordinates cell growth, autophagy and metabolism. Nat. Cell Biol. *13*, 1016–1023.

Niewiadomski, P., Kong, J.H., Ahrends, R., Ma, Y., Humke, E.W., Khan, S., Teruel, M.N., Novitch, B.G., and Rohatgi, R. (2014). Gli protein activity is controlled by multisite phosphorylation in vertebrate Hedgehog signaling. Cell Rep. *6*, 168–181.

Petrenko, N., Chereji, R.V., McClean, M.N., Morozov, A.V., and Broach, J.R. (2013). Noise and interlocking signaling pathways promote distinct transcription factor dynamics in response to different stresses. Mol. Biol. Cell *24*, 2045–2057.

Phoenix, K.N., Devarakonda, C.V., Fox, M.M., Stevens, L.E., and Claffey, K.P. (2012). AMPKα2 Suppresses Murine Embryonic Fibroblast Transformation and Tumorigenesis. Genes Cancer *3*, 51–62.

Rohatgi, R., Milenkovic, L., and Scott, M.P. (2007). Patched1 regulates hedgehog signaling at the primary cilium. Science *317*, 372–376.

Sanders, M.J., Grondin, P.O., Hegarty, B.D., Snowden, M.A., and Carling, D. (2007). Investigating the mechanism for AMP activation of the AMP-activated protein kinase cascade. Biochem. J. *403*, 139–148.

Sasaki, H., Hui, C., Nakafuku, M., and Kondoh, H. (1997). A binding site for Gli proteins is essential for HNF-3beta floor plate enhancer activity in transgenics and can respond to Shh in vitro. Development *124*, 1313–1322.

Scott, J.W., Oakhill, J.S., and van Denderen, B.J. (2009). AMPK/SNF1 structure: a menage a trois of energy-sensing. Front. Biosci. (Landmark Ed.) *14*, 596–610.

Steinberg, G.R., and Kemp, B.E. (2009). AMPK in health and disease. Physiol. Rev. *89*, 1025–1078.

Suter, M., Riek, U., Tuerk, R., Schlattner, U., Wallimann, T., and Neumann, D. (2006). Dissecting the role of 5′-AMP for allosteric stimulation, activation, and deactivation of AMP-activated protein kinase. J. Biol. Chem. *281*, 32207–32216.

Teperino, R., Amann, S., Bayer, M., McGee, S.L., Loipetzberger, A., Connor, T., Jaeger, C., Kammerer, B., Winter, L., Wiche, G., et al. (2012). Hedgehog partial agonism drives Warburg-like metabolism in muscle and brown fat. Cell *151*, 414–426.

van der Velden, Y.U., Wang, L., Zevenhoven, J., van Rooijen, E., van Lohuizen, M., Giles, R.H., Clevers, H., and Haramis, A.P. (2011). The serine-threonine kinase LKB1 is essential for survival under energetic stress in zebrafish. Proc. Natl. Acad. Sci. USA *108*, 4358–4363.

Viollet, B., Athea, Y., Mounier, R., Guigas, B., Zarrinpashneh, E., Horman, S., Lantier, L., Hebrard, S., Devin-Leclerc, J., Beauloye, C., et al. (2009). AMPK: Lessons from transgenic and knockout animals. Front. Biosci. (Landmark Ed.) *14*, 19–44.

Wang, Y., Ding, Q., Yen, C.J., Xia, W., Izzo, J.G., Lang, J.Y., Li, C.W., Hsu, J.L., Miller, S.A., Wang, X., et al. (2012). The crosstalk of mTOR/S6K1 and Hedgehog pathways. Cancer Cell *21*, 374–387.

Wick, A.N., Drury, D.R., Nakada, H.I., and Wolfe, J.B. (1957). Localization of the primary metabolic block produced by 2-deoxyglucose. J. Biol. Chem. *224*, 963–969.

Wilding, M., Coppola, G., Dale, B., and Di Matteo, L. (2009). Mitochondria and human preimplantation embryo development. Reproduction *137*, 619–624.

Xiao, B., Heath, R., Saiu, P., Leiper, F.C., Leone, P., Jing, C., Walker, P.A., Haire, L., Eccleston, J.F., Davis, C.T., et al. (2007). Structural basis for AMP binding to mammalian AMP-activated protein kinase. Nature *449*, 496–500.

Xiao, B., Sanders, M.J., Underwood, E., Heath, R., Mayer, F.V., Carmena, D., Jing, C., Walker, P.A., Eccleston, J.F., Haire, L.F., et al. (2011). Structure of mammalian AMPK and its regulation by ADP. Nature *472*, 230–233.

Xu, Q., Liu, X., Zheng, X., Yao, Y., Wang, M., and Liu, Q. (2014). The transcriptional activity of Gli1 is negatively regulated by AMPK through Hedgehog partial agonism in hepatocellular carcinoma. Int. J. Mol. Med. *34*, 733–741.

Yang, J.Y., Zong, C.S., Xia, W., Yamaguchi, H., Ding, Q., Xie, X., Lang, J.Y., Lai, C.C., Chang, C.J., Huang, W.C., et al. (2008). ERK promotes tumorigenesis by inhibiting FOXO3a via MDM2-mediated degradation. Nat. Cell Biol. *10*, 138–148.

Yang, W., Park, I.J., Yun, H., Im, D.U., Ock, S., Kim, J., Seo, S.M., Shin, H.Y., Viollet, B., Kang, I., et al. (2014). AMP-activated protein kinase α2 and E2F1 transcription factor mediate doxorubicin-induced cytotoxicity by forming a positive signal loop in mouse embryonic fibroblasts and non-carcinoma cells. J. Biol. Chem. *289*, 4839–4852.